AD-A159 429 MICRON-SPACED PLATINUM INTERDIGITATED ARRAY ELECTRODE: 1/1
FABRICATION THEORY.. (U) NORTH CAROLINA UNIV AT CHAPEL
HILL DEPT OF CHEMISTRY R W MURRAY SEP 85 TR-16
UNCLASSIFIED N00014-82-K-0337 F/G 9/1 NL

END
FILMED
DTIC

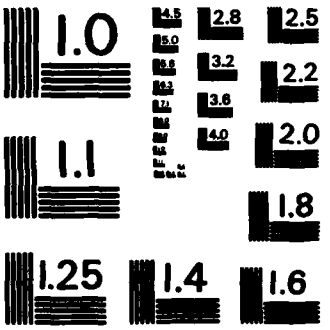

MICROCOPY RESOLUTION TEST CHART
NATIONAL BUREAU OF STANDARDS - 1963 - A

(2)

OFFICE OF NAVAL RESEARCH

Contract N00014-82-K-0337

TECHNICAL REPORT # 16

Micron-Spaced Platinum Interdigitated Array Electrode: Fabrication, Theory and Initial Use

by

Royce W. Murray, Principal Investigator

Department of Chemistry

University of North Carolina

Chapel Hill, North Carolina 27514

Prepared for publication in Analytical Chemistry

REPORT DOCUMENTATION PAGE

READ INSTRUCTIONS BEFORE COMPLETING FORM

1. REPORT NUMBER: Technical Report #16	2. GOVT ACCESSION NO.: A159 429
3. RECIPIENT'S CATALOG NUMBER:	
4. TITLE (and Subtitle): Micron-Spaced Platinum Interdigitated Array Electrode: Fabrication, Theory and Initital Use	5. TYPE OF REPORT & PERIOD COVERED:
	6. PERFORMING ORG. REPORT NUMBER:
7. AUTHOR(s): Christopher E. Chidsey, B. J. Feldman, C. Lundgren, and Royce W. Murray	8. CONTRACT OR GRANT NUMBER(s):
9. PERFORMING ORGANIZATION NAME AND ADDRESS: Department of Chemistry, University of North Carolina, Chapel Hill, NC 27514	10. PROGRAM ELEMENT, PROJECT, TASK AREA & WORK UNIT NUMBERS:
11. CONTROLLING OFFICE NAME AND ADDRESS: Office of Naval Research, Department of the Navy, Arlington, Virginia 22217	12. REPORT DATE: SEPT. 85
	13. NUMBER OF PAGES:
14. MONITORING AGENCY NAME & ADDRESS(if different from Controlling Office):	15. SECURITY CLASS. (of this report): Unclassified
	15a. DECLASSIFICATION/DOWNGRADING SCHEDULE:

16. DISTRIBUTION STATEMENT (of this Report)

Approved for Public Release, Distribution Unlimited

17. DISTRIBUTION STATEMENT (of the abstract entered in Block 20, if different from Report)

18. SUPPLEMENTARY NOTES

19. KEY WORDS (Continue on reverse side if necessary and identify by block number)

micron-spaced platinum electrode, (IDA), microlithographic

micrometer

20. ABSTRACT (Continue on reverse side if necessary and identify by block number)

An interdigitated array (IDA) electrode composed of 40 pairs of 0.3μm thick Pt fingers 3.5μm wide and separated by 2.5μm gaps of insulating borosilicate glass substrate has been fashioned by a modified microlithographic technique. The two IDA is applied to measurement of redox electron conduction through films of poly-$[Os(bpy)_2(vpy)_2](ClO_4)_2$, poly-$[Ru(bpy)_2(vpy)_2](ClO_4)_2$, and Prussian Blue that had been electrochemically deposited over the Pt fingers and in the insulating gaps. Appropriate theory for using the IDA for this purpose is developed. Electrochemically generated luminescence from solutions of $Ru(bpy)_3^{2+}$ is also observed with the IDA.

DD FORM 1 JAN 73 1473 EDITION OF 1 NOV 65 IS OBSOLETE

SECURITY CLASSIFICATION OF THIS PAGE (When Data Entered)

Micron-Spaced Platinum Interdigitated Array Electrode: Fabrication, Theory and Initial Use

Christopher E. Chidsey

AT&T Bell Laboratories

Murray Hill, New Jersey 07974

B. J. Feldman, C. Lundgren, and Royce W. Murray

Department of Chemistry

University of North Carolina

Chapel Hill, NC 27514

BRIEF

An interdigitated array (IDA) electrode composed of 40 pairs of 0.3μm thick Pt fingers 3.5μm wide and separated by 2.5μm gaps of insulating borosilicate glass substrate has been fashioned by a modified microlithographic technique.

Micron-Spaced Platinum Interdigitated Array Electrode: Fabrication, Theory and Initial Use

Christopher E. Chidsey

AT&T Bell Laboratories

Murray Hill, New Jersey 07974

B. J. Feldman, C. Lundgren, and Royce W. Murray

Department of Chemistry

University of North Carolina

Chapel Hill, NC 27514

ABSTRACT

An interdigitated array (IDA) electrode composed of 40 pairs of 0.3μm thick Pt fingers 3.5μm wide and separated by 2.5μm gaps of insulating borosilicate glass substrate has been fashioned by a modified microlithographic technique. The two IDA is applied to measurement of redox electron conduction through films of poly-$[Os(bpy)_2(vpy)_2](ClO_4)_2$, poly-$[Ru(bpy)_2(vpy)_2](ClO_4)_2$, and Prussian Blue that had been electrochemically deposited over the Pt fingers and in the insulating gaps. Appropriate theory for using the IDA for this purpose is developed. Electrochemically generated luminescence from solutions of $Ru(bpy)_3^{2+}$ is also observed with the IDA.

Micron-Spaced Platinum Interdigitated Array Electrode: Fabrication, Theory and Initial Use

Christopher E. Chidsey

AT&T Bell Laboratories

Murray Hill, New Jersey 07974

B. J. Feldman, C. Lundgren, and Royce W. Murray

Department of Chemistry

University of North Carolina

Chapel Hill, NC 27514

Electrochemically reactive materials have received considerable research attention over the past several years. A substantial variety of materials have been identified to be sufficiently conductive of both electrons and ions as to allow electrochemical charging as films in contact with electrodes (1). Possible applications include, among many, electrocatalysis (2), chemical sensing (3), information display (3-5) and energy storage (6,7).

Measurement of the electron and ion transport properties of these electroactive materials is an important step in their rational utilization and modification. We and others have examined (1,8-17) the transport properties of a number of polymeric electroactive materials using a variety of electrochemical techniques. One class of electrochemical techniques measures ion transport and is exemplified by our work with "ion gates" (8). Another type can be called charging rate measurements; these sample simultaneous electron and ion motion over macroscopic distances and are typified by

potential step chronocoulometry of thin redox polymer films on planar electrodes (9,10).

A third type of electrochemical technique samples electron conduction in the absence of macroscopic ion motion. Such measurements are made in a cell which allows steady-state electron flow through the electroactive polymer film. Steady-state conditions were originally achieved with a rotating disk electrode coated with the electroactive polymer and immersed in a solution of a non-permeating redox mediator (11-13). More recently, microstructures allowing two electrodes to contact a polymer film have been developed (14). The idea is to measure the steady state current flow between the two electrodes as a function of the average oxidation state of the polymer.

Electrode/polymer/electrode microstructures have been developed in two forms. The first approach, called a "sandwich electrode" (15), used a porous (evaporated) gold overcoat on top of a polymer film that had been deposited on a solid platinum electrode.

We employ in this paper, a second approach using sputtered film, interdigitated platinum electrodes spaced 2.5 μm apart on an insulating substrate. Below, we describe the fabrication of this microstructure, which is an example of an "array electrode" (16,17). The two electrode pattern was defined by a microlithographic process. The purpose of the interdigitated array (IDA) pattern (see Fig. 1) is to maximize the length of the 2.5 μm insulating corridor bounded by the two electrodes.

Microlithography, by now a well established tool in electronics, has not been extensively used in chemical research. There are two notable recent applications. The first is the use of microlithographically defined structures in the fabrication of chemical sensors (18). Particularly interesting has been the work of Wohltjen and coworkers with surface acoustic wave (SAW) devices

made with interdigitated gold electrodes on quartz substrates (18), which can be used to sense and measure adsorbates on the device surface. The second recent application of microlithography was the fabrication by Wrighton and coworkers (16,17) of diode and transistor structures by combining polypyrrole and related electroactive polymers with arrays of microlithographically defined gold electrodes.

Platinum has long been a favored electrode material with electrochemists. Its stability at positive potentials is of particular significance in our laboratory because many of the electroactive polymers we study exhibit oxidations at potentials more positive than 1.0V vs. SSCE. Ironically, the chemical stability of Pt also makes it a difficult material to pattern with standard techniques. To our knowledge, no well-behaved chemical etch of thin Pt films is available for micro-patterning using conventional photoresist techniques (19). An alternating current electrochemical etch based on alternate cycles of oxide reduction followed by Pt oxidation and dissolution in 3M HCl has been developed (20), but we found it unsatisfactory for our pattern due to both electrode resistance and resist undercutting. Instead, we adopted the Ar^+ sputter-etching technique described below which gave excellent patterning with our arrays.

An alternative to patterning by etching is the so-called "lift-off" technique in which the metal film is deposited over an organic resist pattern. Dissolution of the resist can lead to lift-off of the undesired metal. This approach was the basis for the Wrighton group's patterning of Au (17), but to our knowledge has not yet been described for Pt.

This paper also reports application of the Pt IDA we have fabricated to measurement of the electron conduction properties of poly-$[Os(bpy)_2(vpy)_2]^{2+}$, poly-$[Ru(bpy)_2(vpy)_2]^{2+}$, and Prussian Blue electroactive polymer films

deposited on the IDA. We further present theory appropriate for interpreting these measurements, which give the electron conduction in terms of an electron diffusion coefficient D_e.

It is important that the reader appreciate the distinction between electron conduction measurements on electroactive polymeric materials using array (IDA) or sandwich electrodes, and those more classical conduction measurements made with dry compressed pellets between electrode sandwiches or with four point probe arrangements on dry film materials (21,22). First, it is a fundamental characteristic of electroactive polymers that they exhibit ion conduction as well as electron conduction since a change in their electrochemical redox state require, for electroneutrality, a concurrent change in the number of charge compensating counterions. Thus, the experimental arrangement often requires provision for contact of the polymer with an electrolyte solution. Secondly, the electron conduction, depending on the electroactive material and the experimental arrangement, may be either potential gradient-driven (23), or it may be driven by a concentration gradient of oxidized and reduced states, corresponding to "electron diffusion" or redox conduction (15). In either case, the conductivity may vary considerably with the material's oxidation state. Thirdly, measuring redox conduction (D_e) driven only by concentration gradients, without interference from superposition of appreciable potential gradients, is best done on rather thin polymer films (down to 100 nm); these can be difficult to mechanically contact in a controlled manner. Consequently, the more classical approaches to measuring electron conduction may not be readily applied to interesting aspects of electron conduction in electroactive polymers.

IDA electrodes have analogy to other electrode designs used in electrochemistry besides the sandwich electrode (15) and additionally can be

used to study solutions of electroactive species. An IDA in contact with a solution of an electroactive solute is somewhat similar to a twin electrode thin layer cell, TETLC (24). One of the two closely spaced electrodes can be poised at an oxidizing potential to generate oxidized species, which diffuse to the other electrode where they can be reduced. (In this case the vertical walls of the Pt fingers act as the two electrodes of a TETLC.) The resulting steady state current can be a sensitive measure of either the concentrations or diffusion constants of electroactive solutes. Similar analogy may be made between an IDA and a rotated disk electrode (25), a rotated ring-disk electrode (25) and a microelectrode (26); all are ways to obtain steady-state mass transport to an electrode surface. We illustrate the application of the Pt IDA to a solution reaction by observing electrochemically generated luminescence from the $[Ru(bpy)_3]^{2+}$ system.

EXPERIMENTAL

2"x2"x0.032" barium borosilicate glass substrates (Corning 7059) were rinsed with a pressurized jet of distilled water, sonicated in isopropanol for 15 minutes and suspended over refluxing isopropanol for 12 hours. 1000Å of Ti was deposited from below onto one face of each substrate at about 2Å/s in a liquid nitrogen-trapped vacuum chamber. The Ti source was a resistively heated Ti wire coil about 6" from the substrate. The chamber was heated and gettered by sublimation of several thousand Angstroms of Ti before a shutter protecting the substrates was opened to start the deposition at about 5×10^{-7} torr. The substrates were transferred in air to a liquid nitrogen-trapped magnetron sputtering chamber (Polaron) in which 2,000Å of Pt was deposited at about 2Å/s from a pre-sputtered foil target. The bias was 2.6 kV and the sputtering gas was Ar at about 80 mtorr.

The metallized substrates were coated with about 1.2 μm of Shipley 1470 positive photoresist and photolithographically patterned by Sentek Inc. (P.O. Box 18000, Orlando, FL 32880, 305-888-8860), using a GAM device photomask generously loaned to us by D. Bolioso and H. Woltjen of the Naval Research Laboratory. The substrates were then scribed and broken into pieces small enough to fit in a small ion-beam etching system. After a spray rinse with H_2O and an air bake at 120°C for 30 min., the pieces were sputter etched at normal incidence for 45 min. with 70 $\mu A/cm^2$ of 1 kV Ar^+ ions from a Commonwealth ion gun. Next, the pieces were wet etched at 60°C for 5 min. in a Ti etching solution of 100g H_2O:10g 30% H_2O_2 in H_2O:4g ethylenediaminetetraacetic acid (H_4EDTA):4g 30% NH_4OH in H_2O. The resist film was removed in an oxygen plasma (100 mtorr O_2 gas in a Harrick plasma cleaner at full r.f. power for 45 min.). These glass pieces were coated with a photoresist film to protect the surface, mounted on a glass block with rubber cement and cut into individual IDA regions with a metallographic diamond saw. There were 192 individual IDA regions on each 2"x2" glass substrate, and there are 40 Pt fingers (20 connected to each contact pad) in each of the IDA regions used in this paper.

The separated IDA regions were electrically tested for shorts between the electrodes by contacting the pads with sharp probes. IDA regions that were not shorted were mounted as shown in Fig. 2. (A substantial fraction of those which were shorted could be opened by applying 20-40 VAC between the pads, which was effective at melting tiny, shorting Pt filaments. Sometimes, the presence of larger shorting Pt filaments in the gaps also led during application of 20-40VAC to the melting of one or both fingers connected to the shorting filament. Since such devices still contained an adequate number of working finger pairs, and since the effect of the reduced number of fingers could be accounted for by theory (vide infra), such devices were used.) The

IDA's were attached with Scotch 5-min epoxy to cylindrical mounts (Buehler casting epoxy) containing two copper leads. The assembly was then washed in photoresist developer or methyl ethyl ketone to remove the protective resist coating. Each copper lead was connected to one of the electrodes of the IDA with indium metal applied with a hot soldering iron. The Cu and In were coated with 5-min epoxy, and all exposed 5-min epoxy was painted with Apeizon vacuum wax dissolved in cyclohexane. The remaining "contact pad" area of the Pt electrodes was also coated with Apiezon wax so that only the Pt "fingers" were left exposed (Figure 1). This mounting procedure is exacting and was mostly done with the aid of a stereoscopic microscope.

Electrochemical instrumentation, cells, electrolytes and metal polypyridine compounds were all similar to those previously described (27). Prussian blue films were deposited electrochemically by a procedure similar to that of Itaya (28,29), but at constant potential rather than current. An SLM fluorimeter was used to detect electrogenerated chemiluminescence through a double monochromator with "photon-counting" detection. Optical microscopy was with a Zeiss Universal Microscope.

RESULTS AND DISCUSSION

IDA Fabrication. Both the initial titanium and overlying Pt films had mirror surfaces both to the naked eye and under a microscope. Ti provides an excellent adhesive layer between glass and Pt, and its adherent, insoluble surface oxide makes any exposed areas innocuous except under special chemical conditions (HF, EDTA or other strong chelating agents).

Following the photoresist lithographic patterning, the exposed Pt and underlying Ti films are to be removed to create the insulating gap regions. This was done by ion beam etching of the Pt. From changes in interference

colors, it was clear that, at the ion dose used, the resist layer was also thinned by the ion beam but that a uniform organic film remained, effectively masking the desired areas of Pt which would form the IDA fingers. Ti sputters much more slowly than Pt; so a wet Ti etch was necessary to avoid sputtering through the rest of the organic resist layer.

After O_2 plasma-stripping of the resist, optical microscopy showed a featureless mirror finish of the Pt fingers in the protected areas and clean featureless glass in the unprotected area. The Pt fingers were 3.5 μm wide with 2.5 μm gaps between them. The photoresist pattern was reproduced with nearly perfect fidelity except for occasional spots that should have been etched but appear to have been protected from the sputter etching by small adherent particles.

Electrical testing showed that an appreciable fraction of the interdigitated electrodes were shorted. In one batch of 192 IDA's only 20 were open. Microscopic examination of shorted IDA's invariably revealed at least one unetched spot of Pt (~3μm in diameter) bridging the electrodes. The shadowing particulates which probably cause these spots are likely created in the scribing and breaking steps needed to reduce the size of the 2" substrates. If so, the yield of initially good IDA's should greatly improve if scribing and breaking could be avoided. As noted in Experimental, many of the shorted IDA's could be opened by application of 20-40 VAC between the contact pads.

A sensitive measure of the nature of a Pt surface is its cyclic voltammogram in 1M H_2SO_4 (30). Fig. 3 shows the first and fifth potential scans of one set of fingers of a mounted IDA starting at 0V vs. SSCE. The reduction peak at +0.5V is due to Pt oxide stripping. The nearly reversible peaks at -0.03 and -0.12V are due to Pt hydride, and the sharp increase in cathodic current at -0.2V is due to H_2 discharge. The sharpening of these

features on repeated scanning indicates that contaminants are being removed, probably by oxidation at positive potentials. Three anodic features are present in the positive potential scans. Beginning at +0.6V positive there is the broad plateau due to Pt oxide formation. The broad current rise around +1.0V which disappears on scanning is probably due to the oxidation of organic contaminants. Finally, the sharp increase in anodic current is due to further Pt oxidation and O_2 discharge. There is a cathodic offset in the so-called "double layer" region between the oxide stripping and hydride features that is probably due to reduction of O_2 dissolved in the electrolyte. Our conclusion is that these electrodes are tolerant of and can be easily cleaned by brief cycling in acid. At that stage they act chemically like bulk, polycrystalline Pt (30).

IDA Use with Redox Polymers. Metal Poly-Pyridines Films and Theory. To explore the utility of our IDA electrode for the study of redox polymers, we chose first to look at thin films of poly-$[M(bpy)_2(vpy)_2](ClO_4)_2$ where M = Os or Ru, bpy = 2,2'-bipyridine and vpy = 4-vinylpyridine. Thin films were formed from acetonitrile solutions of the monomer complexes by reductive electropolymerization in the same manner as previously reported (27). The potentials of both electrodes of an IDA immersed in a solution of the monomer were scanned together repeatedly at 0.1 V/s through a negative potential range spanning the two reduction features of the bipyridine ligands.

Microscopic examination of the resulting Os polymer-coated electrodes showed a film over the region of interdigitated Pt fingers that spread about 10-20 μm beyond the outermost Pt fingers. The film was a uniform, fairly transparent coating speckled with a few dark spots about 1 μm in diameter. A similar morphology has been noted before in this laboratory for this polymer on

large-area, polished Pt surfaces. Given these observations we believe that the polymer film is deposited uniformly over both fingers and gaps.

The Os(III/II) electrochemistry of a poly-$[Os(bpy)_2(vpy)_2](ClO_4)_2$ film on an IDA in a solution of 0.1M Et_4NClO_4 in CH_3CN is presented in Fig. 4. Fig. 4A shows the cyclic voltammetry with the potentials of both Pt electrodes scanned together as a common working electrode (with reference and auxiliary electrodes elsewhere in the solution). Note the nearly symmetric anodic and cathodic peaks with little peak-to-peak splitting; these are features characteristic of surface-bound redox species undergoing rapid electron transfer with the electrodes (1). Fig. 4B shows a four electrode experiment in which the potential of Pt Electrode 1 is swept and that of Pt Electrode 2 is held at 0V vs. SSCE. The potential scan rate is one tenth that in Fig. 4A. The currents at the two electrodes, i_1 and i_2, are mirror images of one another, since they reflect steady state responses attributable to concentration gradient driven electron conduction from one electrode to the other across the poly-$[Os(bpy)_2(vpy)_2]^{2+/3+}$ film in the insulating gap. Note that the half-maximal value of i_2 occurs at the same potential as the current peaks in Fig. 4A. This is expected (27) and is $E^{o'}$ for the Os(III/II) couple. The hysteresis in the i_1 traces is due primarily to the small polymer charging current needed to change the average oxidation state of the film as the potential is swept past $E^{o'}$. Qualitatively, these features are entirely analogous to those observed with the same polymer in sandwich electrodes (27), where the interelectrode spacing is about ten times less than the IDA.

Quantitative analysis of Fig. 4 allows a determination of the electron diffusion coefficienc $D_e(III/II)$ for the Os(III/II) mixed-valent state of the polymer. We present the necessary theory for this next.

Initially, conduction through a polymer film overlaid onto an IDA would appear to present a complex geometrical problem. There is however, a physically reasonable limiting case which is quite simple. Consider the cartoon of Fig. 5, showing a partial cross-section of an IDA coated uniformly with polymer of thickness $\underline{t}$. The polymer thickness $\underline{t}$ shown in the Figure is less than the height $\underline{h}$ of the Pt fingers, so that ideally, the IDA experiment is simply an "open face sandwich" electrode where the area of the electrode/polymer interface on either side of the sandwich is the product $\underline{lt}$ where $\underline{l}$ is the length of the two Pt fingers. Consequently, the equation for the limiting electron conduction current $(i_L)_{segm}$ across the gap of dimension $\underline{d}$ is, for one two finger segment,

$$(i_L)_{segm} = n\,F\,lt\,D_e C_s/d \qquad (1)$$

where C_s is the Os redox site concentration. The total charge Q_{segm} (as collected in a slow potential scan cyclic voltammogram for exhaustive oxidation or reduction of the polymer) for a two finger segment of the IDA is

$$Q_{segm} = n\,F\,lp\,t\,C_s \qquad (2)$$

where p is the center-to-center width of the two finger segment. Combining Eqns. 1 and 2, we obtain a relation for the electron diffusion coefficient

$$D_e = \frac{dp\,(i_L)_{segm}}{Q_{segm}} = \frac{i_L\,dp}{Q} \cdot \frac{N}{N-1} \qquad (3)$$

in which the ratio, i_L/Q, of the total current (i_L) and charge (Q) observed with the array is taken to be the same as the ratio $(i_L)_{segm}/Q_{segm}$ for a single two finger segment. If there are $\underline{N}$ fingers in the IDA, the correction factor $(\underline{N}/\underline{N}-1)$ accounts for the fact that Q includes the charge for polymer coated on the outermost halves of the two outermost fingers, but the polymer there does not contribute to any of the electron conduction. This factor would be significant for arrays with small numbers of fingers (16,17).

There are several other conditions relevant to the above relations. (i) Strictly, Eqn. 1 requires that $\underline{t} \leq \underline{h}$. This requirement is relaxed however, if the gap dimension $\underline{d}$ greatly exceeds the film thickness $\underline{t}$. That is, approximate adherance to Eqn. 1 can be obtained for $\underline{t} > \underline{h}$ provided that $\underline{d} \gg \underline{t}$. (ii) The distance $\underline{s}$ away from the Pt fingers where uniform polymer deposition occurs (in an electropolymerization experiment) should be large compared to the gap dimension, $\underline{d}$, so that a uniform film exists in the gap, yet (iii) the distance $\underline{s}$ should not be so large that the polymer deposited on the glass beyond the outermost fingers of the array contributes significantly to $\underline{Q}$.

The dimensions for the IDA used in this work are given in Figure 5. The overall array dimensions are 0.24 cm ($\underline{l}$) for the finger lengths and 0.024 cm for the array width ($\underline{N}$ = 40 fingers x $\underline{p}$ = 6×10^{-4} cm center-to-center finger distance). For the poly-$[Os(bpy)_2(vpy)_2](ClO_4)_2$, $\underline{s}$ = 10-20 μm (*vide supra*), which is greater than the 2.5μm gap dimension $\underline{d}$. For the poly-$[Os(bpy)_2(vpy)_2](ClO_4)_2$ coated IDA used in Fig. 4, Q = 3.4μC, i_L = 0.41μA, and C_s = 1.5$\underline{M}$ (27). The average thickness of the film, $\langle\underline{t}\rangle$, can be written:

$$\langle t\rangle = Q/(nFC_s lpN) = 0.041\mu m \qquad (4)$$

which is less than the finger height, 0.3μm. Assuming for the moment that the polymer film is uniform (e.g., $t = \langle t\rangle$), we conclude that the model of Fig. 5 and Eqn. 3 are applicable to our data.

Eqn. 3 is remarkably simple. It depends on the number of fingers, N, in the IDA only in the (N/N-1) correction factor. For large N this factor is near unity. (In our array, N = 40 when all Pt fingers are completely functional.) Having large N also increases the absolute values of i_L and Q, making measurement easier. Secondly, the length l of the array does not appear, which is a convenience when using procedures like the wax masking of the end sections used here, since sometimes the edges are irregular. Thirdly, the concentration of redox sites C_e and the film thickness t do not appear. This feature is unique to this approach to measuring D_e, since other known procedures (10,10,15,27) require some estimate of these quantities, and thus of film swelling. In the "closed face" sandwich electrode, for instance, the relation for D_e analogous to Eqn. 3 would be (27)

$$D_e = \frac{i_L t^2}{Q} = \frac{i_L Q}{C_e^2} \qquad (5)$$

Using Eqn. 3 and results like those of Fig. 4, three different IDA measurements on the Os(III/II) wave of poly-$[Os(bpy)_2(vpy)_2](ClO_4)_2$ films gave $D_e(III/II) = 1.8\times10^{-8}$, 1.1×10^{-8}, and 3.0×10^{-8} cm^2/s, or an average $D_e(III/II) = 2.0 \pm 0.7\times10^{-8}$ cm^2/s. This is about three times larger than previous results for $D_e(III/II)$ in this polymer obtained from "closed face" sandwich electrodes, $8 \pm 3\times10^{-9}$ cm^2/s (27).

Poly-$[Ru(bpy)_2(vpy_2)](ClO_4)_2$ films were also deposited on IDA electrodes. Although the amount of polymer on the electrode is comparable to that used with Os, no micro-sized specks were microscopically observed. The electrochemistry of the Ru(III/II) wave was very similar to that observed in Fig. 4 for the Os

polymer. (Because it is necessary to scan to ca. 1.3V vs. SCE in acetonitrile to observe Ru(III/II) voltammogram, this measurement could not have been accomplished with a Au array.) $D_e(III/II)$ values of 1.1×10^{-8} and 1.2×10^{-8} cm^2/s were obtained from films on two different IDA's. These Ru polymer values are a factor of two smaller than that for the Os polymer. This result is in distinct contrast to the results obtained with sandwich electrodes where $D_e(III/II)$ was found to be seven times greater for the Os polymer than for the Ru polymer (27).

The redox conduction supported by the bipyridine redox waves of the poly-$[Os(bpy)_2(vpy)_2](ClO_4)_2$ and poly-$[Ru(bpy)_2(vpy)_2](ClO_4)_2$ films was also measured. As has been observed before for the Os polymer (27), the reduced states (labelled Os(I), Os(0), Ru(I) and Ru(0) for convenience) are unstable and repeated potential cycling through these states leads to a decreased electron conductivity. Thus only lower limits on the initial limiting currents for the Os(II/I), Os(I/0), Ru(II/I) and Ru(I/0) mixed-valent states could be obtained. From these we conclude that the ratios of D_e values for the Os and Ru polymers, $D_e(III/II):D_e(II/I):D_e(I/0)$, are 1: >3: >42 and 1: >3: >20, respectively. These results are very similar to those results obtained from sandwich electrodes for the Os polymer (27), where the ratios were determined to be 1: >3: >25.

It appears from the above results that the absolute values of electron diffusion coefficients obtained with the Pt IDA (e.g., $D_e(III/II)$ may be systematically larger than those obtained with older methods. Let us consider the possible reasons for this difference. First, consider the microscopic observation of 1 μm dark specks on the poly-$[Os(bpy)_2(vpy)_2](ClO_4)_2$ film (vide supra). If these specks are polymer dendrites, they would contribute to the charge, Q, measured in Fig. 4A but not to the limiting current i_L measured in

Fig. 4B. By this reasoning Eqn. 3 would underestimate D_e, which is in the wrong direction to account for the discrepancy. Secondly, the sandwich (and other) measurements of D_e depend (Eqn. 4) on C_s, the concentration of metal complex sites in the polymer, whereas Eqn. 3 for the IDA does not. An overestimation of C_s would decrease the calculated sandwich D_e but would not affect the IDA result. This is in the correct direction to produce the observed difference. However, profilometry on this polymer produces estimated (dry) thicknesses within 20-30% of those calculated from the polymer density, and microscopic observation of a small, wetted particle shows little dimensional change. We believe that any errors in C_s are not logically large enough to account for the present discrepancy. Thirdly, fabrication of the sandwich structure requires condensation of a metal vapor onto the outer surface of the polymer film. This has the potential of damaging the film and decreasing its electron conduction properties. The IDA structure is completely formed before film deposition, and electron conduction can be measured immediately after film deposition without any intervening treatments. We consider this a possible explanation for the discrepancy in D_e. Lastly, whereas the sandwich electrode (and other methods) samples the entire polymer film electropolymerized on the metal surface by electron transport normal to the surface during electropolymerization, the IDA structure measures electron conduction laterally through a polymer film that has been deposited more remotely from the metal surface, in the insulating gap. It is quite possible, then, that the microscopic morphology of the two kinds of deposited polymers may differ in a manner making the IDA-prepared material more conductive. We can only speculate about this last possibility at present.

Prussian Blue Films. Films of insoluble metal cyano complexes have captured increasing interest (28,31-33) since Neff's original report (34) that films of an iron cyano complex (Prussian Blue) could be formed on electrodes and were electroactive. These materials have ostensibly more ordered internal structures than most electroactive polymer films, (35)and afford an important opportunity for study of electron transport in relation to the transport of charge compensating counterions through the lattice. There have been two attempts at measurement of electron transport in Prussian Blue (36,37); the chronoamperometric results of Viehbeck and DeBeny (36) are the more correctly interpreted and indicate that $D_e = 5\times10^{-9}$ and 2.7×10^{-9} cm^2/s for reduction and oxidation, respectively. However, neither measurement was under steady state current flow conditions where difficulties with gross ohmic potential gradients and macroscopic counterion transport are minimized. Prussian Blue films seemed, accordingly, a timely object of IDA experiments.

The Prussian Blue films were formed onto the array by application of 0.5V vs. SCE (to both Pt fingers) in a solution containing 2 mM $K_3Fe(CN)_6$, 2 mM $FeCl_3$, 0.01M KCl, and 0.01 M HCl. The thickness of the films, which were visibly blue as formed, was regulated by the time of potentiostating (or better, by the amount of charge passed), and was selected (38) to give films less than 0.3μm thick as confirmed by profilometry. Microscopically, they were smooth and uniform although the thicker films showed evidence of fissures characteristic of shrinking and cracking upon drying. (Presently, as a precaution, the films are not allowed to dry.) We have not carried out compositional analysis of these films but presume at this point that they are mostly $[Fe_4(Fe(CN)_6)_3]$, but probably also contain some defect structures such

as $K[Fe(Fe(CN)_6)]$. Water is also presumed to be a film constituent both from previous Prussian Blue crystallography (35) and because we have ascertained (38) that in gas phase ion budget (39) experiments, water is an essential ingredient to electron conduction.

The Prussian Blue films exhibit two cyclic voltammetric waves in 0.5 M KCl (aq.), at about 0.2V and at 0.9V vs. SCE, which represent the oxidation state changes of the low and high spin iron states in the inorganic film (5), respectively. The cyclic voltammetry of the 0.2V wave is illustrated in Fig. 6. This voltammogram was obtained by scanning both sets of Pt fingers in the IDA together (as was done in Fig. 4A). The voltammetric shape is similar to that reported by Neff (5,34,37). We believe this wave actually represents as many as three overlapping waves, at ca. 0.33V, at 0.2V (the main feature), and at ca. 0.1V. The charge under the overall wave is 58μC, which corresponds to a film containing 1.3×10^{-7} eqv./cm^2 of electroactive sites.

Fig. 7 shows the same Prussian Blue film where the potential of one electrode of the array is scanned from 0.5V to -0.2V vs. SCE and back (the current flowing at this electrode is the upper trace), while the potential of the other Pt electrode is held, at +0.5 V (lower current trace). The potential scan is sufficiently rapid that the central feature of the cyclic voltammogram (see Fig. 6) is clearly visible in the current response of the electrode whose potential is swept; it is the transient current required to change the oxidation state of the Prussian Blue film. (At sufficiently slow sweep rate, the peak should disappear.) The approach to steady state is rapid enough within the film-coated gap region that very little hysteresis is evident in the current measured at the other, constant potential Pt electrode. Clearly

defined, equal, and oppositely signed limiting current plateaus are seen at both Pt electrodes.

Application of Eqn. 3 to the limiting current (i_L = 1.95 μA) of Fig. 7, using the charge (Q = 58 μC) under the entire cyclic voltammetric wave in Fig. 6, gives a $D_e = 5.0 \times 10^{-9}$ cm^2/s for the electron diffusion coefficient through this $Fe^{II}Fe^{III} + e^- \rightarrow Fe^{II}Fe^{II}$) mixed valent form of Prussian Blue. The average of four experiments gave $D_e = 2.8 \pm 1.1 \times 10^{-9}$ cm^2/s. (This is in good agreement with the previous chronoamperometric result (36); however, see below.) D_e is unchanged if the same experiment is done in KNO_3 electrolyte. Further IDA experiments in different electrolytes and solvents, on the more positive voltammetric wave for Prussian Blue, and under ion budget (39) control are on-going (38), and will be reported separately. Arriving at a molecular interpretation of D_e, as for other electroactive polymers (1), will depend on discerning whether intrinsic electron self-exchange rates, lattice dynamics, or correlated counterion hopping constitutes the main activation barrier for the electron diffusion process. The interpretative problem is complicated by the following significant feature of the IDA voltammetry of Fig. 7.

Ideally, the half-maximal current of a DC electron conduction voltammogram occurs at the formal potential $E^{o'}$ of the redox couple constituting the mixed valent state. This was the case as we noted above for the poly-$[Os(bpy)_2(vpy)_2](ClO_4)_2$ film in Fig. 4. Careful examination of Fig. 7 (lower trace) shows, however, that the half-maximal DC conduction current ($i_L/2$, see dashed line) occurs at 0.14V (average of forward and reverse scans), which is more negative than the major, sharp voltammetric feature at 0.2V (Fig. 7 upper trace, and Fig. 6). It appears in fact that the DC electron conduction through the Prussian Blue film is associated mostly with the shoulder wave at ≈ 0.14V

in Fig. 6. Use of the total charge Q = 58 μC under the reduction peak(s) in Fig. 6 to calculate D_e from Eqn. 3 is consequently somewhat misleading. Experiments (38) aimed at estimating D_e as a more precise function of film oxidation state suggest in fact that the D_e associated with the ~0.14V shoulder wave is over 10x larger than that of the main, sharp 0.2V voltammetric feature. Previous discussions (5,28,34,37) have implicitly presumed that the Prussian Blue voltammetry corresponds to "one kind" of iron site electroactivity; these results show clearly that this is not the case.

We do not have a complete explanation for the different electron conductivities in Prussian Blue revealed by Figure 7, but believe the following points will have to be considered in its explanation. Firstly, previous studies (35) show that the ideal formula of Prussian Blue contains 3/4 of the high spin iron coordinated to four cyano nitrogens and two waters whereas the remainder are coordinated to six cyano nitrogens. These sites may have intrinsically different formal potentials as a result. Alternatively, the high spin iron sites may have initially similar $E^{o'}$, but because of site-site interactions (such as occur in biferrocenes) some of the sites become non-equivalent upon reduction of the others. In either case, the resultantly different iron sites can exhibit differing D_e as a result of differing barriers to electron hopping between them, or as a result of differing barriers for motions of the charge compensating counterions that are associated with the different iron species. Secondly, the Prussian Blue materials probably contain numerous crystal defects which may strongly influence the ion and electron motions. These are difficult topics, but are the subjects of some present experiments (38).

Other Uses of IDA Electrodes. The geometry of the IDA electrodes should be

useful for a number of other types of electrochemical measurements besides electron transport in redox polymer films. We have recently become interested in the highly energetic reaction between M(III) and M(I) states that occurs when a potential difference of more than 2.1 V is used to cause (ion budgeted) conduction through dry films of poly-$[M(bpy)_2(vpy)_2](ClO_4)_2$ (39). A valuable probe of this chemistry would be measurement of any excited state luminescence, which would be a form of electrochemically generated luminescence (ECL) (40). Unfortunately, the sandwich structure used in the early (39) ion budget experiments precluded optical observation of the film. An IDA electrode should allow such experiments. As a prelude to such a study, we have looked at the related but much more fully studied case of ECL from $[Ru(bpy)_3](ClO_4)_2$ dissolved in an electrolyte solution in contact with the IDA (41,42).

Figure 8A shows the cyclic voltammetry of 1.2 mM $[Ru(bpy)_3]^{2+}$ in 0.1M Et_4NClO_4/CH_3CN measured by scanning both electrodes of the IDA together. The potential separations of the anodic and cathodic peaks of each feature (60-80 mV) are typical of freely diffusing redox species at large-area electrodes. The "diffusion profile averaging time" for gold minigrid electrodes with 6.4 μm gaps has been demonstrated to be aout 10 ms (43) which is fast on the timescale of Fig. 8A. Accordingly, at potential scan rates of 100 mV/s, we expect these IDA electrodes, when the Pt fingers are scanned together, to act like one large-area electrode. Fig. 8B shows the near steady state current observed at one of the electrodes if its potential is swept while the other electrode is held at OV vs. SSCE. The behavior is qualitatively identical to what is observed with a twin electrode thin layer cell [21]; the electrode held at OV is bathed in the diffusion profile of products of the electrolysis at the swept electrode. No luminescence is observed in either Fig. 8A or 8B.

Fig. 8C shows an analogous experiment, sweeping the potential of one electrode and now holding the potential of the other Pt finger at +1.3 V vs. SSCE. Luminescence is now observed as shown by the dotted line. At the electrode held at +1.3 V, $[Ru(bpy)_3]^{2+}$ is oxidized to $[Ru(bpy)_3]^{3+}$. When the other electrode attains sufficiently negative potentials to reduce $[Ru(bpy)_3]^{2+}$ to $[Ru(bpy)_3]^{1+}$, the reduced and oxidized species formed at the two electrodes diffuse together and an electron is transferred in a very exothermic reaction ($\Delta G = 2.6$ eV). Luminescent excited states are formed, and light is emitted (41,42).

Though the gross features of Fig. 8 are readily interpreted, quantitative aspects of these experiments have not been fully explored. It was not our present aim to attempt quantitative study, since this chemistry has been well examined by others (41,42). Our aim is to illustrate and explore the use of the IDA geometry. In the future, we hope to adapt the ECL experiment to redox polymer films.

Other uses of IDA electrodes include ion budgeted electrochemical studies in the absence of solvent (39) and we have found (38) that such experiments are possible. The combination of "dry" electrochemistry and the planar geometry of the IDA may also allow valuable tools like X-ray fluorescence and photoelectron spectroscopy to be applied to a functioning electrochemical cell. A related frontier which should be explored is the micropatterning of the electroactive polymer films as well as the electrodes. To date, studies of these polymers on array electrodes have exploited the morphology characteristic of the electrodeposited polymer. In the future, techniques such as UV crosslinking, electron beam-induced depolymerization, "lift-off" patterning, masked etching etc. may prove useful in creating interesting polymer-polymer junctions. Much

conceptual groundwork for such structures lies in previous studies from this laboratory on "bilayer" electrodes (14,44), and Kittleson, et al (45) have in fact recently achieved a bilayer-type polymer/polymer junction using an array electrode.

Acknowledgement. This research was supported in part a grant from the Office of Naval Research. The authors are grateful to Dr. Debra Rolison of the Naval Research Laboratory for helpful discussions at the inception of this research, to Dr. H. Wohltjen of NRL for generous loan of the photomask used for our array and for the gift of an example Au finger array, and to Professor T. Meyer of this Department for use of ion sputtering apparatus.

1. Murray, R. W., Ann. Rev. Mate. Sci. 1984, 14, 145.
2. Collman, J. P.; Denisevich, P.; Konai, Y.; Marrocco, M.; Koval, C.; Anson, F. C., J. Am. Chem. Soc. 1980, 102, 6027.
3. Willman, K. W.; Murray, R. W., J. Electroanal. Chem. 1982, 133, 211.
4. Nicholson, M. M.; Pisarello, F. A., J. Electrochem. Soc. 1981, 128, 1760.
5. Ellis, D.; Eckhoff, M.; Neff, V. D., J. Phys. Chem. 1981, 85, 1225.
6. Seeger, R. G.; MacDiarmid, A. G., "The Physics and Chemistry of Low Dimensional Solids", L. Alacer, Ed., 353-397, P. Reidel, 1980.
7. Neff, V. D.; J. Electrochem. Soc., 1985, 132, 1382.
8. Burgmayer, P.; Murray, R. W., J. Phys. Chem. 1984, 88, 2515.
9. Oyama, N.; Anson, F. C., J. Electrochem. Soc. 1980, 127, 640.
10. Facci, J. S.; Schmehl, R. H.; Murray, R. W., J. Am. Chem. Soc. 1982, 104, 4959.
11. Lewis, N. S.; Wrighton, M. S., J. Phys. Chem. 1984, 88, 2009.
12. Ikeda, T.; Leidner, C. R.; Murray, R. W., J. Electroanal. Chem., 1982, 138, 343.
13. Leidner, C. R.; Murray, R. W., J. Am. Chem. Soc. 1984, 106, 1606.
14. Chidsey, C. E. D.; Murray, R. W., Science (1985) submitted.
15. Pickup, P. G.; Murray, R. W., J. Am. Chem. Soc., 1983, 105, 4510.
16. White, H. S.; Kittlesen, G. P.; Wrighton, M. S., J. Am. Chem. Soc. 1984, 106, 5375.
17. Kittlesen, G. P.; White, H. S.; Wrighton, M. S., J. Am. Chem. Soc. 1984, 106, 7389.
18. Wehltjen, H., Anal. Chem. 1984, 56, 87A.
19. Thin Film Processes, Vossen, J. L.; Kern, W.; Eds., Academic Press, New York, 1978.
20. Frankenthal, R. P.; Eaton, D. H., J. Electrochem. Soc. 1976, 123, 703.
21. Pittman, C. U.,; Surynarayanan, B., J. Am. Che. Soc. 1974, 96, 7916.
22. Shriver, D. F.; Papke, B. L.; Ratner, M. A.; Dupon, R.; Wong, T.; Brodwin, M., Solid State Ionics 1981, 5, 83.
23. Feldman, B. J.; Burgmayer, P.; Murray, R. W., J. Am. Chem. Soc. 1985, 107, 872.
24. Anderson, L. B.; Reilley, C. N., J. Electroanal. Chem. 1965, 10, 295.
25. Bard, A. J.; Faulkner, L. R., Electrochemical Methods: Fundamentals and Applications, Wiley, New York (1980).
26. Howell, J. O.; Wightman, R. M.; Anal. Chem. 1984, 56, 524.
27. Pickup, P. G.; Kutner, W.; Leidner, C. R.; Murray, R. W., J. Am. Chem. Soc. 1984, 106, 1981.
28. Itaya, K.; Ataka, T.; Toshima, S., J. Am. Chem. Soc. 1982, 104, 4767.
29. Lundgren, C.; Murray, R. W., unpublished results, Univ. of North Carolina, 1985.
30. Ross, P. N. Jr., J. Electrochem. Soc. 1979, 126, 67.
31. Bocarely, A. B.; Sinha, S., J. Electroanal. Chem. 1982, 137, 157.
32. Crumbliss, A. L.; Lugg, P. G.; Morosoff, N., Inorg. Chem. 1984, 23, 4701.
33. Schneemeyer, L. F.; Spengler, S. E.; Murphy, D. W., Inorg. Chem., submitted.
34. Neff, V. D., J. Electrochem. Soc. 1978, 125, 886.
35. Buser, H. J.; Schwarzenbach, D.; Petter, W.; Ludi, A., Inorg. Chem.

1977, 16, 2704.

36. Viehbeck, A.; DeBerry, D. W., J. Electrochem. Soc. 1985, 132, 1369.

37. Rajan, K. P.; Neff, V. D., J. Phys. Chem. 1982, 86, 4361.

38. Feldman, B. J.; Lundgren, C.; Murray, R. W., unpublished results, Univ. of North Carolina, 1985.

39. Jernigan, J. C.; Chidsey, C. E. D.; Murray, R. W., J. Am. Chem. Soc. 1985, 107, 2824.

40. Faulkner, L. R.; Bard, A. J. in Electroanalytical Chemistry, Vol. 10, ed. A. J. Bard, Marcel Dekker Inc., p. 1.

41. Luttmer, J. D.; Bard, A. J., J. Phys. Chem. 1981, 85, 1155.

42. Glass, R. S.; Faulkner, L. R., J. Phys. Chem. 1981, 85, 1160.

43. Petek, M.; Neal, T. E.; Murray, R. W., Anal. Chem. 1971, 43, 1069.

44. Leidner, C. R.; Denisevich, P.; Willman, K. W.; Murray, R. W., J. Electroanal. Chem. 1984, 164, 63.

45. Kittlesen, G.; White, H.; Wrighton, M. S. J. Am. Chem. Soc., in press.

FIGURE LEGENDS

Fig. 1. Pt finger pattern of IDA. The 2400 μm long central section (between the whitestars) of the array contains the 40 Pt fingers used in this work. The non-interdigitated sections at each end (next to the contact pads) were masked over as part of the IDA mounting (Fig. 2) and are inactive.

Fig. 2. Illustration of the mounting of a typical IDA showing contacts and insulation of the two terminals.

Fig. 3. First and fifth cyclic voltammograms of an IDA electrode where the potentials of both electrodes were scanned together in 1M H_2SO_4 at 100mV/sec.

Fig. 4. Currents from the two sets of Pt fingers, i_1 and i_2, measured during potential sweeps of a poly-$[Os(bpy)_2(vpy)_2](ClO_4)_2$ coated IDA surface in 0.1M Et_4NClO_4/CH_3CN.
Curve A: potentials of both electrodes of the IDA were scanned together at 50mV/sec; the charge under the wave measured 3.4 μC and ΔEp was 0V; Curve B: currents i_1 and i_2 where the potential of electrode #1 was scanned while electrode #2 was held at 0V vs SSCE.

Fig. 5. Cross section of two fingers of an idealized IDA electrode with polymer coating. d=2.5μm, p=6μm, h=0.3μm, f=3.5μm and l is variable, generally

1-2 mm.

Fig. 6. Cyclic voltammogram of a Prussian Blue coated IDA electrode in 0.5M KCl where the potentials of both electrodes were scanned together at 20 mV/sec. The redox wave corresponds to Prussian Blue reduction and reoxidation; the charge under the reduction wave measured 57.8 μC.

Fig. 7. Currents from the two sets of Pt fingers, i_1 and i_2, measured during potential sweeps of a Prussian Blue coated IDA electrode in 0.5M KCl. Upper trace corresponds to cyclical potential sweep of electrode #1 through the Prussian Blue wave of Figure 6, at 5 mV/sec. Lower trace corresponds to the current measured at electrode #2, which was held at 0.5V vs SSCE, during the potential sweep of electrode #1.

Fig. 8. Cyclic voltammograms of an IDA electrode in 1.2mM $[Ru(bpy)_3]^{2+}$/C.1M Et_4NClO_4/CH_3CN. Curve A: The potentials of both sets of Pt finger electrodes were scanned together at 100 mV/sec; Curve B: current measured at electrode #1 the potential of which was scanned at 100 mV/sec while that of electrode #2 was held at 0V vs SSCE; Curve C: Current measured at electrode #1 the potential of which was scanned at 100 mV/sec while that of electrode #2 was held at 1.3V vs SSCE; . . . . represents light emission intensity.

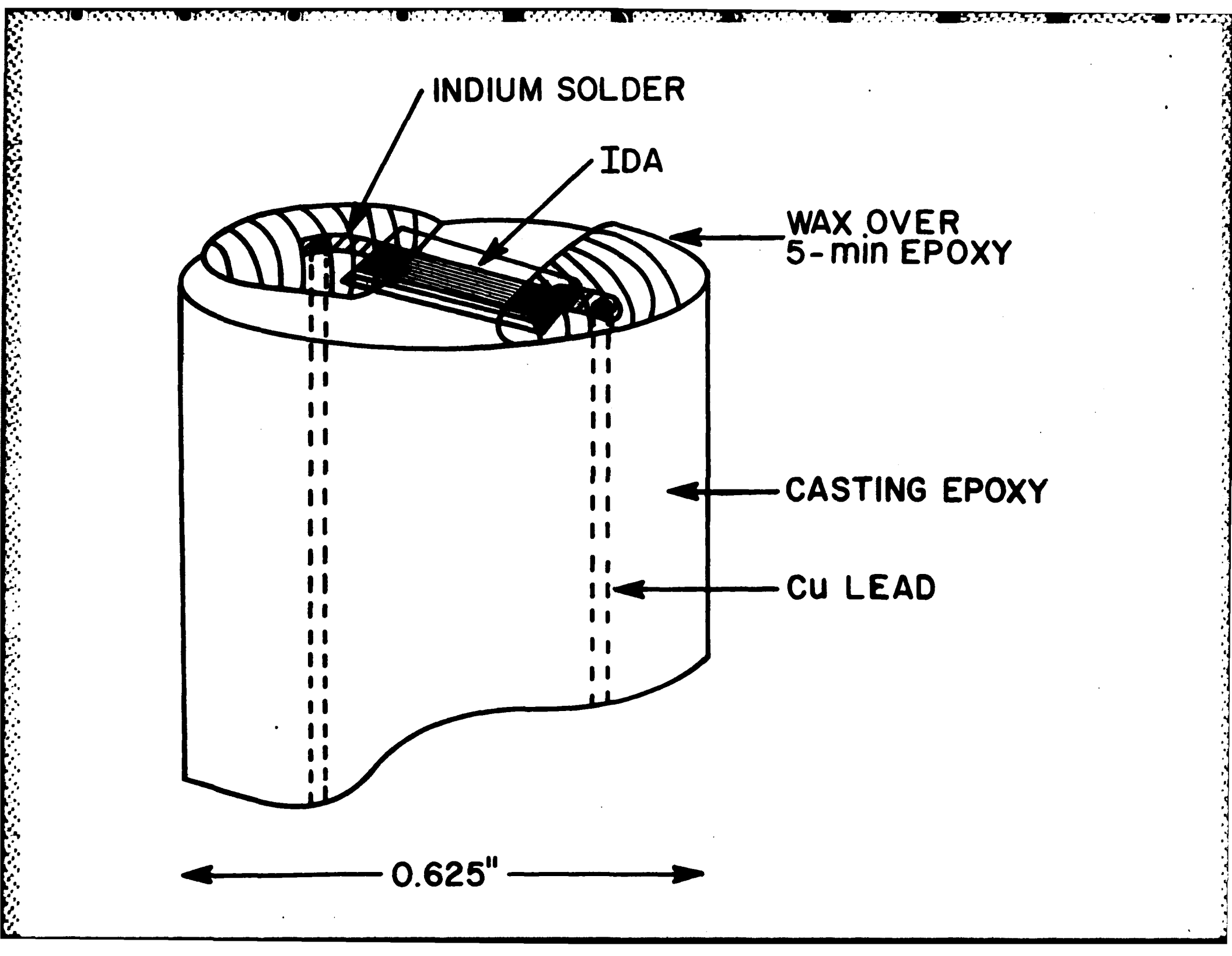
INDIUM SOLDER
IDA
WAX OVER
5-min EPOXY
CASTING EPOXY
Cu LEAD
0.625"

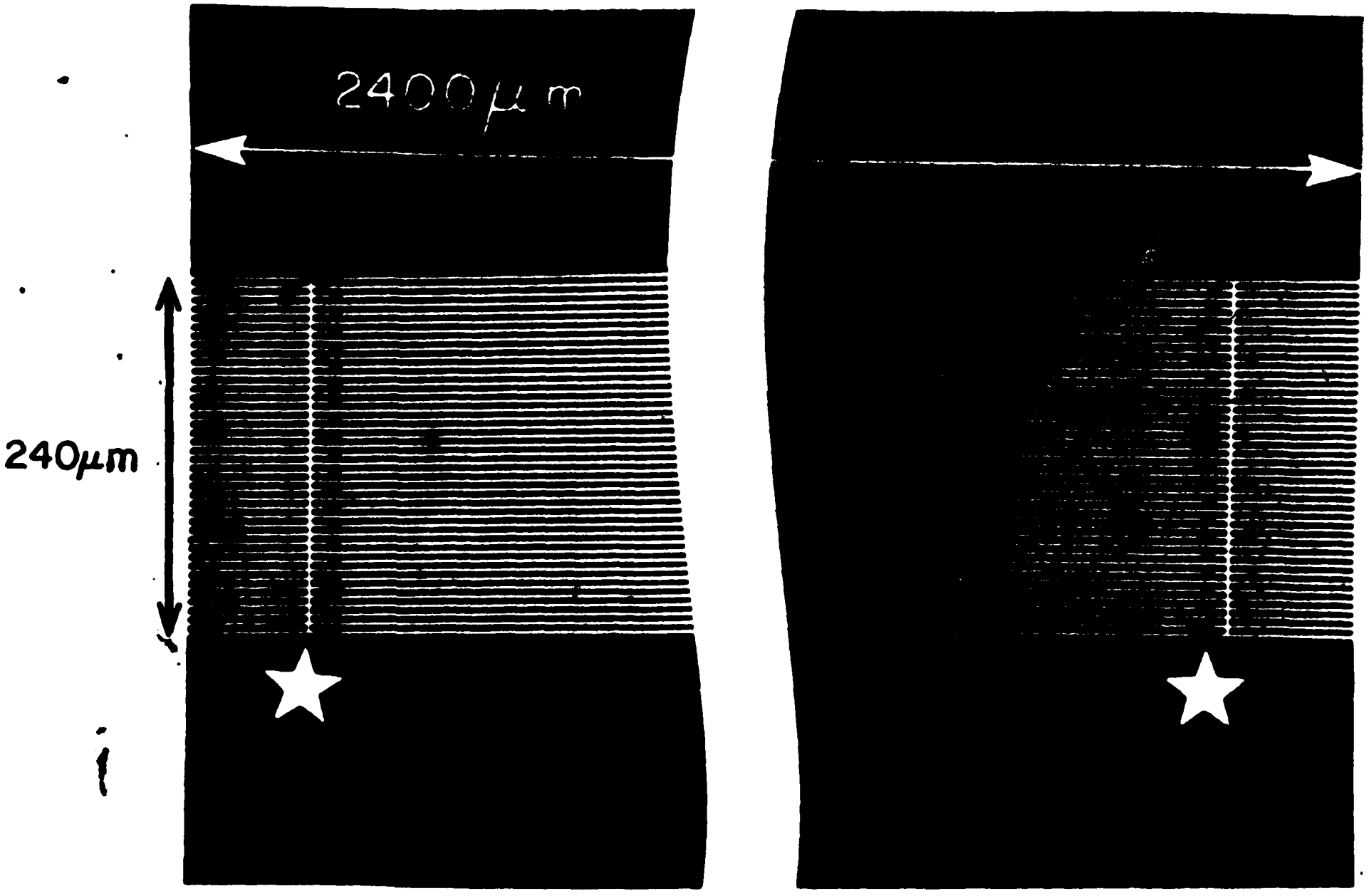
2400μm
240μm

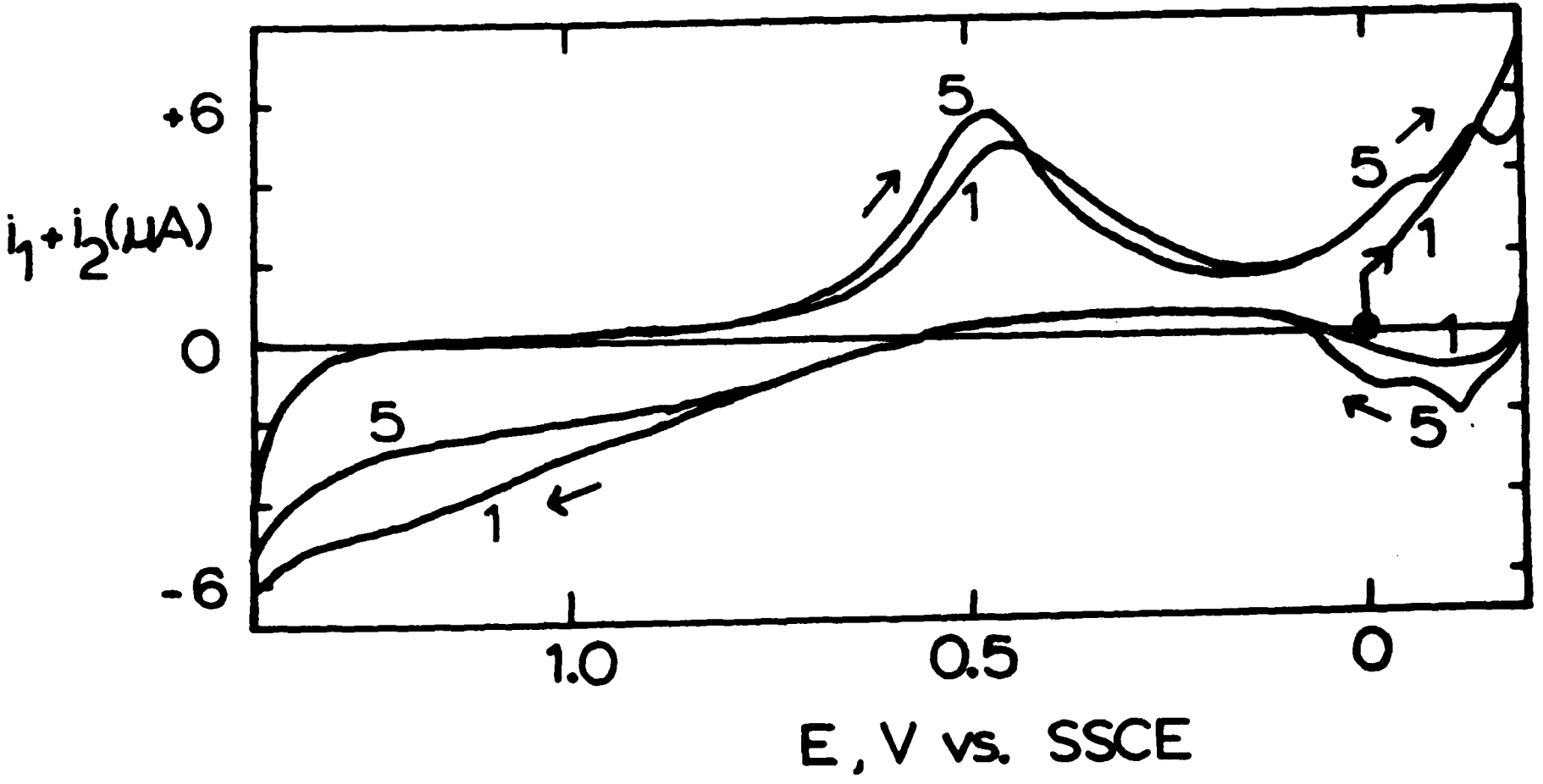
+6
0
-6
$i_1 + i_2$(μA)
5
1
5
1
5
1
5
1
1.0
0.5
0
E, V vs. SSCE

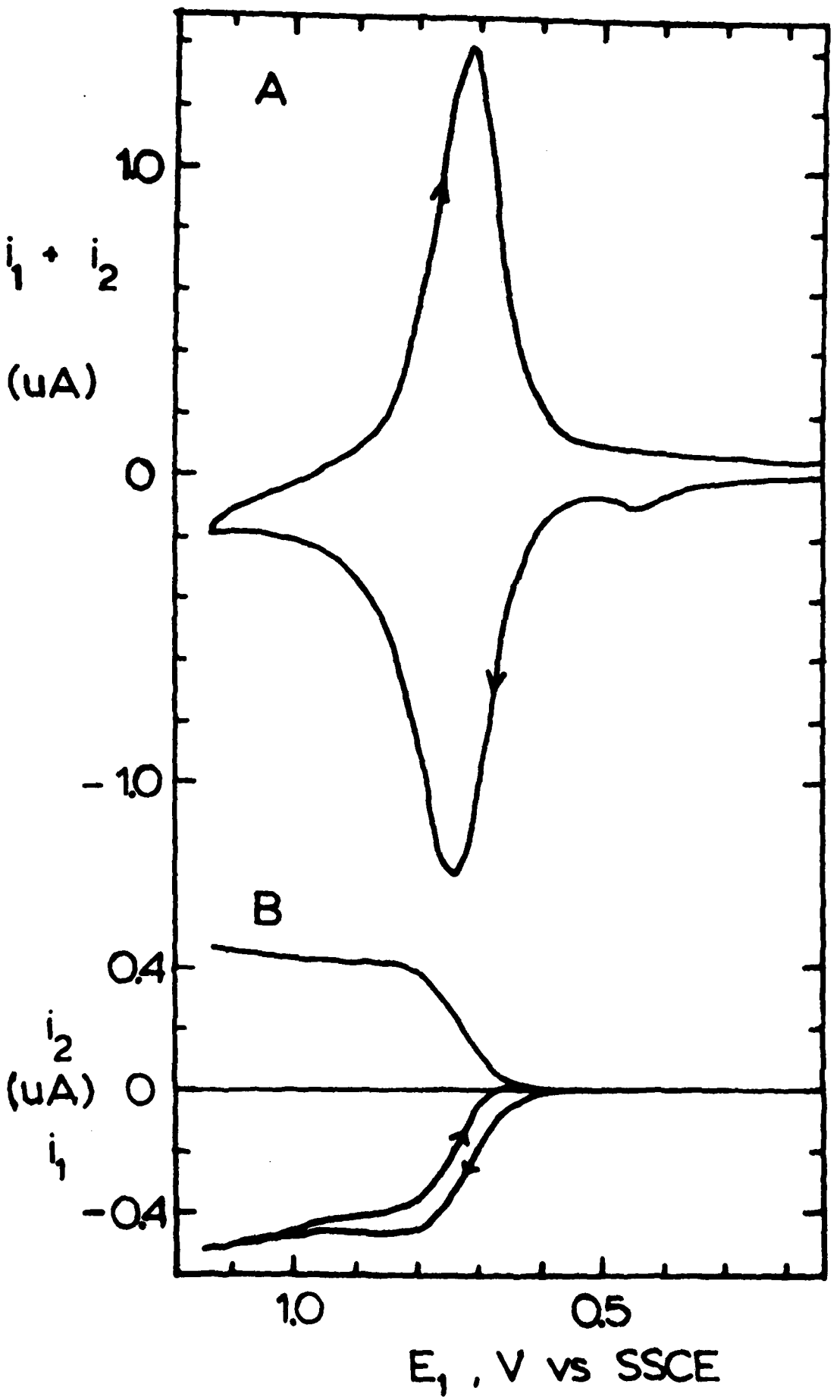
A
1.0
$i_1 + i_2$
(uA)
0
-1.0
B
0.4
i_2
(uA) 0
i_1
-0.4
1.0
0.5
E_1 , V vs SSCE

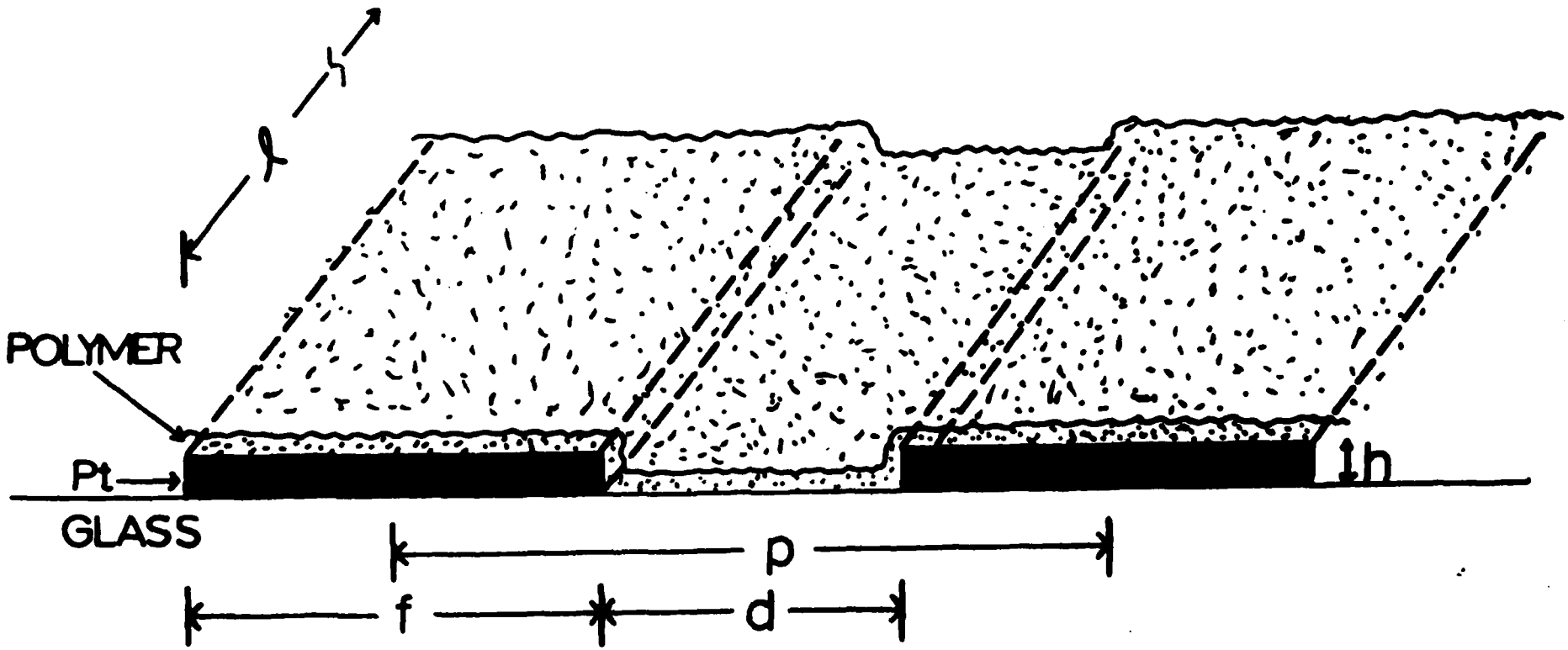

IDEALIZED
OPEN FACE
SANDWICH

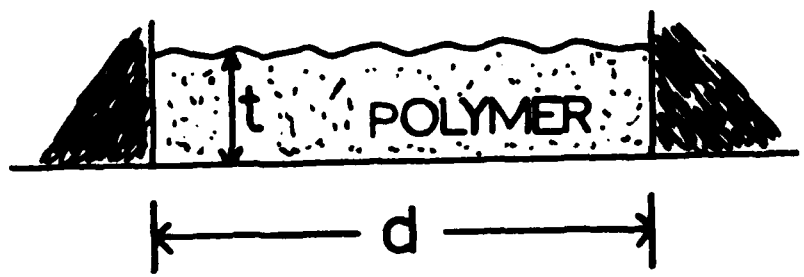

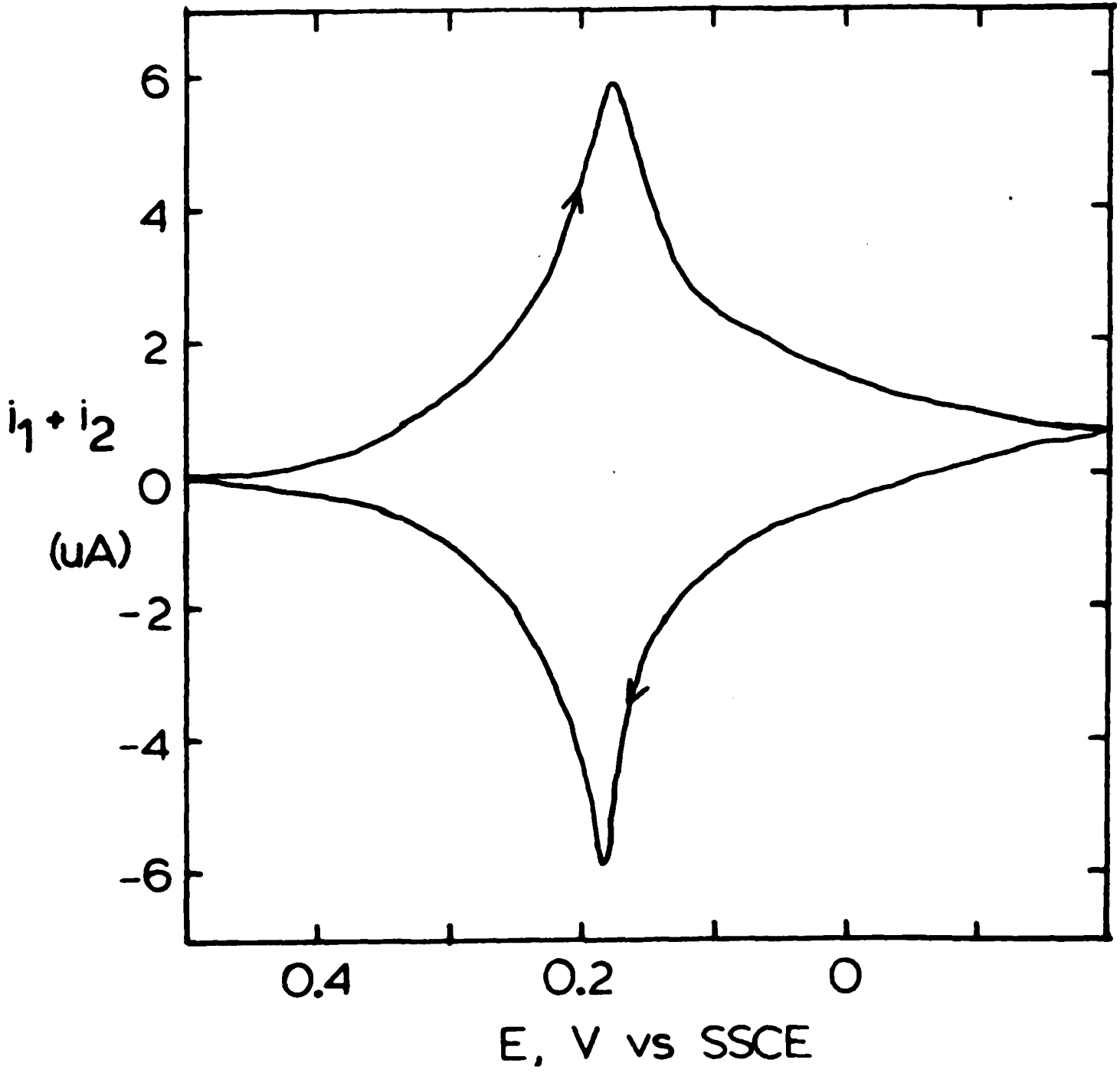
6
4
2
0
-2
-4
-6
$i_1 + i_2$
(uA)
0.4
0.2
0
E, V vs SSCE

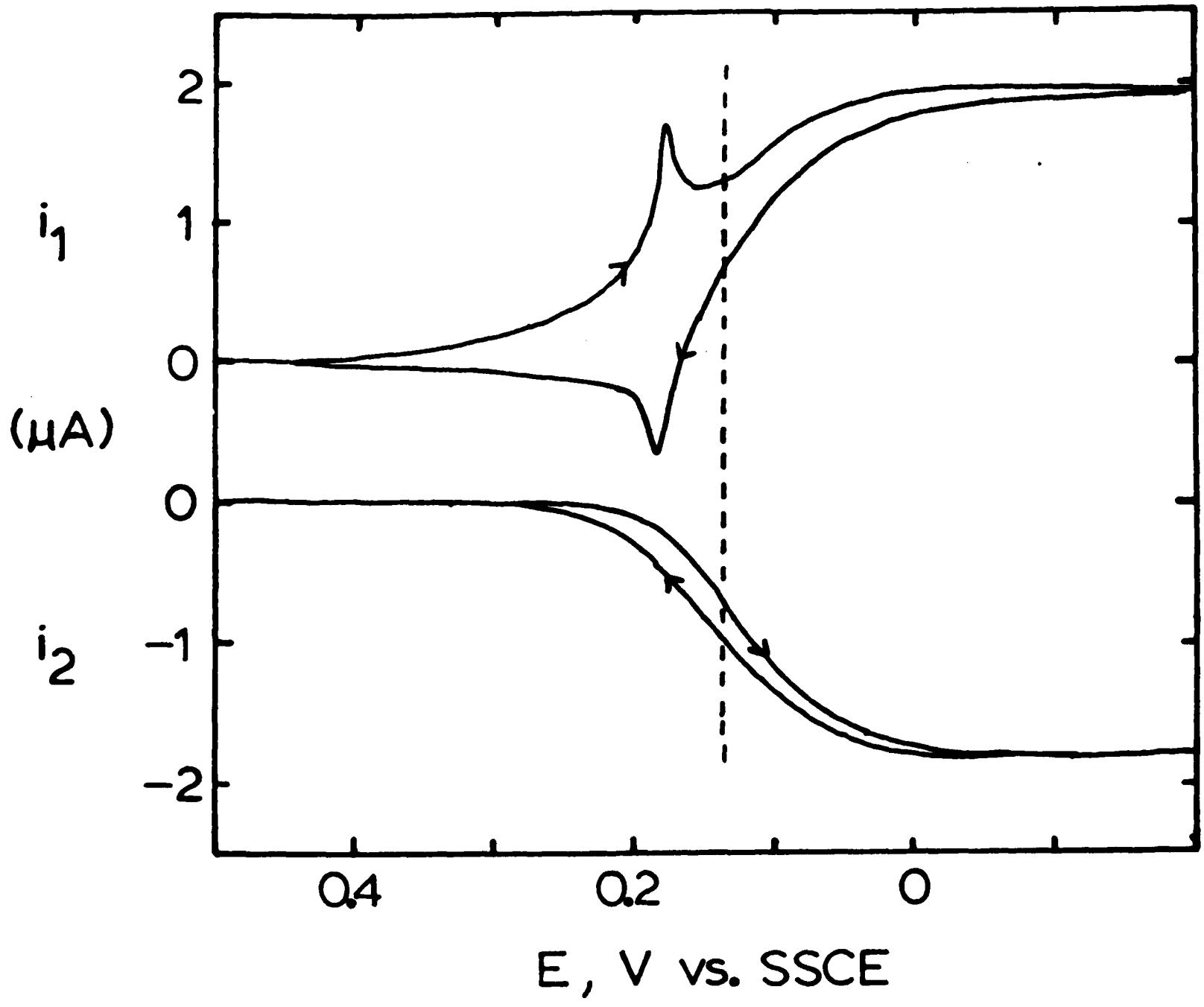
2
1
0
0
−1
−2
i_1
(μA)
i_2
0.4
0.2
0
E, V vs. SSCE

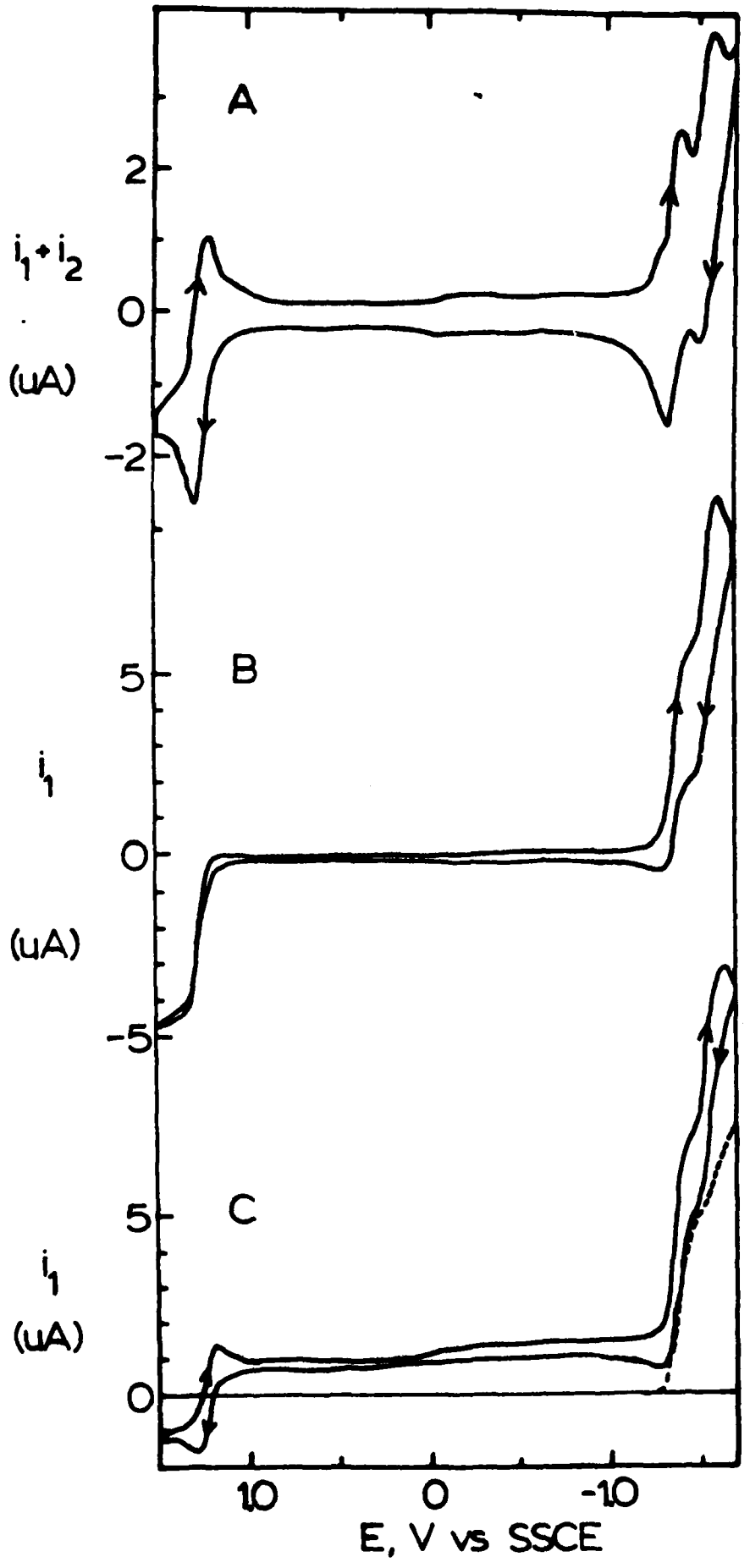
A
2
i_1+i_2
0
(uA)
-2
B
5
i_1
0
(uA)
-5
C
5
i_1
(uA)
0
10
0
-10
E, V vs SSCE

END

FILMED

11-85

DTIC